

Indexed by

Scopus®DOAJ
DIRECTORY OF
OPEN ACCESS
JOURNALS

NUMERICAL INVESTIGATION ON FLEXURAL BEHAVIOR OF RC BEAMS WITH LARGE WEB OPENING EXTERNALLY STRENGTHENED WITH CFRP LAMINATES UNDER CYCLIC LOAD: THREE-POINT BENDING TEST

Crossref**Shahla Abbas Abulqasim**

Civil Engineering
Department, Altinbas
University, Istanbul,
Turkey

Abdul Qader Nihad Noori

Department Civil Engineering,
College of Engineering,
Mustansiriyah University,
Baghdad - Iraq

Tuncer Celik

Civil Engineering
Department, Altinbas
University, Istanbul,
Turkey

ROAD
DIRECTORY OF OPEN ACCESS
RESEARCH RESOURCESKoBSONSCINDEKS
Srpski citatni indeksGoogle
Scholar

Key words: von mises stress, reinforced concrete beam, yielding criteria, carbon fiber reinforced polymer, flexural behavior, cyclic loading, numerical analysis

doi:10.5937/jaes0-32985

Cite article:

Abbas Abulqasim S., Qader Nihad Noori A., Celik T. (2022) NUMERICAL INVESTIGATION ON FLEXURAL BEHAVIOR OF RC BEAMS WITH LARGE WEB OPENING EXTERNALLY STRENGTHENED WITH CFRP LAMINATES UNDER CYCLIC LOAD: THREE-POINT BENDING TEST, *Journal of Applied Engineering Science*, 20(2), 571 - 581, DOI:10.5937/ jaes0-32985

Online access of full paper is available at: www.engineeringscience.rs/browse-issues

NUMERICAL INVESTIGATION ON FLEXURAL BEHAVIOR OF RC BEAMS WITH LARGE WEB OPENING EXTERNALLY STRENGTHENED WITH CFRP LAMINATES UNDER CYCLIC LOAD: THREE-POINT BENDING TEST

Shahla Abbas Abulqasim¹, Abdul Qader Nihad Noori^{2*}, Tuncer Celik¹

¹Civil Engineering Department, Altinbas University, Istanbul, Turkey

²Department Civil Engineering, College of Engineering, Mustansiriyah University, Baghdad - Iraq

In the current paper, the effect of carbon fiber reinforced polymer (CFRP) laminates on the flexural strength of reinforced concrete beam (RCB) with the web opening in the flexural zone was investigated using a numerical method. The main aim of the current work is to model the reinforced concrete beam strengthen by two shape of CFRP laminates (2- layer and U-shape), to observe the influences of CFRP on the flexural strength of the beam. To this end, cyclic loading was applied to investigate the flexural behaviour of the Twelve RC beams under the cyclic loading. All beams kept the same dimensions length, breadth, and depth (2400 × 300 × 200) mm were modeled in the finite elements adopted by ABAQUS software. Steel bars have been used for both flexural strengthening and stirrups. A Three-point bending tests were performed using cyclic loading. Furthermore, the effect of web openings with different sizes (Side length of 40, 60, 75% of the breadth) on the flexural behavior of RC beams was investigated in detail. The flexural strength, local analysis, and ductility of the base beam and CFRP reinforced beam were analyzed. The results of the simulations revealed that the CFRP laminates enhanced the strength of the base beam significantly.

Key words: von mises stress, reinforced concrete beam, yielding criteria, carbon fiber reinforced polymer, flexural behavior, cyclic loading, numerical analysis

INTRODUCTION

In modern construction, it is necessary to create a system of pipes and ducts to provide basic services. These services are water pipes, sewerage, air conditioning, power wiring system, communications, and internet services. Typically, the ducts which have been mentioned are under the slit of the beam and, for aesthetic considerations, they are embraced with a swung roof, forming an unusable room. To optimize the design, it is conventional to use beams with web openings through which these channels can pass, and eventually, it reduces the amount of unused area and as a result, the design is more compressed. This compact design does not demonstrate great savings for usual buildings but in the case of a skyscraper, such a design can have enormous influence as it can reduce the height of the final building by the amount of saving per floor time in the number of floors. This may be one of the most important reasons why web openings have been introduced to the concrete beams [1-8]. Recently the application of fiber-reinforced polymers (FRPs) in civil engineering has risen noticeably due to various advantages of these materials such as low density, high strength to weight ratio, flexibility, comparatively low cost, appropriate durability, and corrosion resistance compared to traditional materials. In the last two decades, the usage of FRP materials for the strengthening of reinforced concrete (RC) has attracted notable attention. Therefore, there have been many studies conducted on the mechanical behavior such as compression, flexural, fatigue, etc. of strengthened sec-

tions by FRP [9-12]. The flexural behavior of reinforced concrete (RC) beams has been studied widely [13-17]. The results of these investigations have revealed the influence of several methods of the FRP system to obtain the needed outcomes. Numerous numerical and experimental studies investigated the effect of different types of strengthening methods in FRP reinforced beams. They have studied different types of FRP materials such as glass, Basalt, carbon, and aramid as well as various shapes of the combination of FRP to the RCs [18-21]. Sonnenschein et al. [22] have investigated the effect of using different FRP composites in the bridge constructions. They reviewed many studies and suggested that steel reinforcement can be substituted with FRP composites specifically when concrete structures subjected to natural environment. They specified that corrosion is the main reason of the failure for the steel reinforcement beams and columns of the bridges, so in these structures FRP can completely satisfied the requirements as a reinforcement instead of traditional reinforcement (steel). They reported the mechanical properties of various types of FRPs and their application in different structural elements of bridges. De Lorenzis et al. [23] compared the behavior of full-scale supported highway bridge deck panels reinforced when bending with either externally bonded CFRP laminates or internally placed NSM CFRP bars. The failure of CFRP laminate reinforced deck covers lies through a combination of tearing and peeling CFRP laminates. NSM CFRP service has been filed tensile rupture of CFRP bars. With respect to

*dr.abdulqadernihad@uomustansiriyah.edu.iq

the ability to unstrengthen deck control, the torque increases from 17 to 29%, the decks are reported to be fitted with externally bonded CFRP laminates and internally placed NSM CFRP bars, respectively. This paper deals with the flexural behavior of Full-scale Reinforced Concrete Beams (RCBs) under the cyclic loading. The RCB specimens contain a large opening (ranged from 40 to 75% of the web depth) at the flexural zone. One solid beam without an opening and strengthening used in this work as a reference specimen. Then adding CFRP laminates to the beams were investigated using ABAQUS software numerically.

Numerical Finite Element Modelling

In the current study, numerical method is utilized to perform the simulation using ABAQUS software[24] that is a well-known and user friend analysis software package which is capable of solving a wide-ranging linear and non-linear problems. Mechanical properties such as density, inelastic and Hashing damage criteria of concrete as well as the mechanical properties of steel and CFRP were defined to model by performing concrete damage plasticity (CDP) model. Isotropic damaged elasticity theory was considered for both compressive and tensile plasticity according to (ABAQUS and Manual 2012)[25]. The parameters related to the CDP FE model have been listed in Table 1 [26]. Uniaxial tensile and compressive

mechanical performances of concrete are needed to characterize the CDP in ABAQUS. The relations for the stress-strain of uniaxial compression test and tensile test are as follows:

$$\sigma_c = E_0 (1 - d_c)(\varepsilon_c - \varepsilon_c^{pl}) \quad (1)$$

$$\sigma_t = E_0 (1 - d_t)(\varepsilon_t - \varepsilon_t^{pl}) \quad (2)$$

Where σ_c , d_c , E_0 , is the compressive stress, compressive damage variable and initial elastic modulus of the material, respectively. Also, σ_t , d_t , E_0 , is the tensile stress, tensile damage variable, respectively. Furthermore, ε_c and ε_c^{pl} are compressive strain and compressive plastic strain, respectively. Also, ε_t and ε_t^{pl} are the strain under the tension and tensile plastic strain, respectively.

Table 1: CDP parameters of Concrete[26]

Dilation Angle (Ψ)	Eccentricity (ϵ)	f_b/f_{c_0}	k	Viscosity (μ)
56	0.1	1.16	0.667	0.0001

The tensile and compression behavior of concrete were defined and utilized for both conditions of prior to ultimate strength and post peak stress. Also, the mechanical properties of CFRP used in the current work is listed in Table 2.

Table 2: Mechanical properties of CFRP [25]

E1 (N/mm ²)	E2 (N/mm ²)	v12	G12 (N/mm ²)	G13 (Nmm ²)	G23 (Nmm ²)
23000	17860	3.0	10000	10000	10000
Longitudinal Tensile Strength (N/mm ²)	Longitudinal Compressive Strength (N/mm ²)	Transverse Tensile Strength (N/mm ²)	Transverse Tensile Strength (N/mm ²)	Longitudinal Shear Strength (N/mm ²)	Transverse Shear Strength (N/mm ²)
3450	2760	133	536	117	117

A developed model by S. Bahij et al. [27-30] has been used in ABAQUS for failure of the concrete. This model has been modified by several researchers. The model offered by Lee et al.[26] was chosen for this study. The plasticity properties may be explained by many phenomena, like strain softening, deterioration of the material gradually, and volumetric expansion, and consequently a decrease in strength and stiffness of the concrete. More details about the CDP model and the related theories is available in the ABAQUS Analysis User's Manual [25]. The plastic properties for stress and strain for damage of the concrete can be achieved by the Equations (3) and (4) to measure damage throughout the degradation only in the softening stage where stiffness is proportional to the cohesion of the sample.

$$\frac{E}{E_0} = \frac{C}{C_{max}} = (1 - d) \quad (3)$$

$$\varepsilon^{-p} = \varepsilon^p - \frac{d}{1 - d} \frac{\sigma}{E_0} \quad \text{and} \quad \varepsilon^{-p} = \varepsilon - \frac{f}{E_0} \quad (4)$$

Where C is cohesion in the criteria of the yield strength, that is also proportional to stress, Cmax is equal to the strength of the concrete, d and f are damage factor and the tensile or compressive strength of concrete. Furthermore, damage compression for model elements and tensile factors is evaluated via Equations (5) and (6), separately.

$$d_c = 1 - \frac{\sigma_c E_c^{-1}}{\epsilon_c^{pl} \left(\frac{1}{bc} - 1 \right) + \sigma_c E_c^{-1}} \quad (5)$$

$$d_t = 1 - \frac{\sigma_t E_c^{-1}}{\epsilon_t^{pl} \left(\frac{1}{bt} - 1 \right) + \sigma_t E_c^{-1}} \quad (6)$$

Where σ_c is the compressive stress and σ_t is tensile stress. E_c is the concrete modulus elasticity, ϵ_t^{pl} is the plastic. The values of bc and bt are recommended by [31] and equal to 0.7 and 0.1, respectively. There are many kinds of tests to determine the flexural strength of a material such as three-point bending and four-point bending tests. In the current work three-point bending tests were simulated in ABAQUS and the schematic of three-point bending test and detailed model used in the simulations is illustrated in Fig.1. Rectangular reinforced beam (RCB) with the width, height and length of 300 mm, 200mm, and 2400 mm, respectively were used as a base model to observe the effect of adding web opening and CFRP on the flexural strength of the beam. Also, the beam was reinforced via 4 bars with the diameters of 8 mm and c/c of 152 mm and series of stirrups with an interval distancing of 100 mm c/c (see Fig. 1). The young modulus of the steel bars and stirrups was defined as 200 Gpa and the mechanical properties of the steel were set in the ABAQUS software. The compressive strength (fc) of the concrete used in the study was 30 MPa.

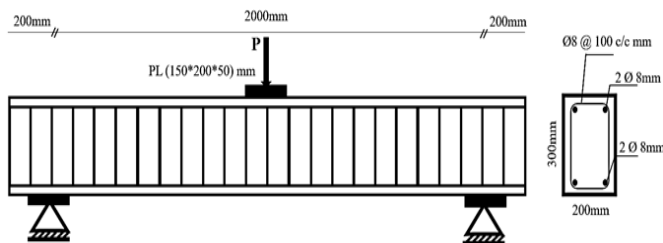


Figure 1: Details of RC beam includes bars and stirrups

The Dynamic behavior of concrete used for the simulation and also damage properties used in ABAQUS for the simulation is presented in Table 3.

Table 3: Dynamic behavior and tensile damage values of concrete used in the simulation

Tensile (CDP)		Tensile Damage		
Stress	in-strain	stress	damage	in-strain
3450652.112	0	3450652	0	0
2295713.038	0.00029	2295713	0.740058	0.00029
1884035.156	0.000549	1884035	0.868129	0.000549
1651583.006	0.000802	1651583	0.916419	0.000802
1496056.714	0.001052	1496057	0.940729	0.001052
1382096.603	0.0013	1382097	0.955019	0.0013

MECHANICAL MODELING

Firstly, the beam, steel embedded region inside of the concrete beam, FRP layers, and rigid bodies for support and applying the deformation were designed in the part module of the ABAQUS software. After that, the material properties of the steel, CFRP, and concrete were defined in the property module. Subsequently, the three-point bending setup was assembled in assembly module of the software as shown in Fig.2.

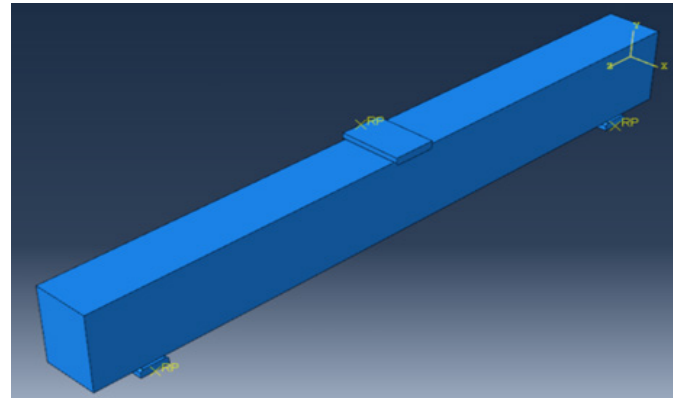


Figure 2: Assembly of the three-point bending system simulated in this study

Also, Fig.3 demonstrates the setup consist of 23 stirrups and 4 steel bars inside of the beam to make the reinforced concrete beam. Furthermore, four rectangular rigid bodies were designed to make the supports at both side of the beam and one for applying the load from the top of the system which can be seen in Fig.3.

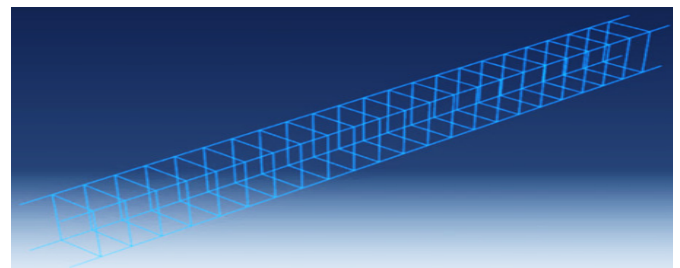
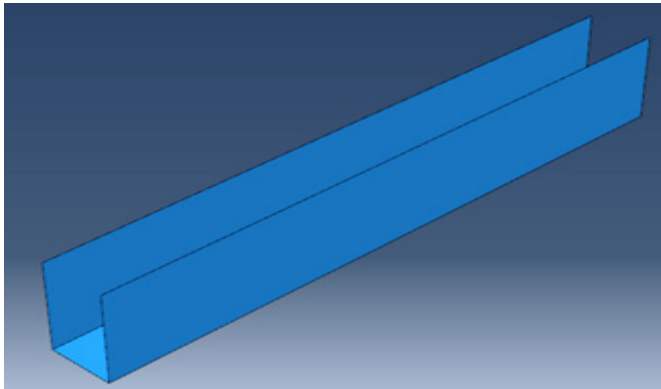
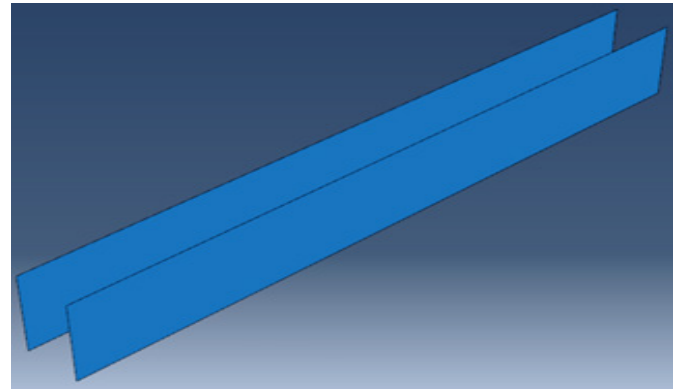


Figure 3: Embedded stirrups and bars of steel



4-a: U shape wrapped CFRP



4-b: CFRP laminated 2- layers

Consequently, U shape and 2-layers wrapped polymer were design to see the effect of CFRP on the flexural strength of the reinforced concrete beams. The design of this laminated layer can be seen in Fig. 4a and 4b For the next part of the modelling in ABAQUS, the interactions between different parts of the system and constraints and contacts were defined. Afterward, in mesh module all the parts were meshed one by one to discretize the parts for numerical solution. Although, low element size may give better results, the low element size increases the number of the elements which subsequently increase the simulation time. Therefore, we have tried to optimize the number of the elements and element size to achieve a reliable result and compute the problem faster. In most of the cases of this thesis, the approximate global size was defined as 0.05. Fig.5 demonstrates the system for the three-point bending test after mesh. Also, The design of CFRP laminates with the thickness of 1 mm and width and length of 300mm and 2400 mm, respectively shown in Fig. 6-a and 6-b.

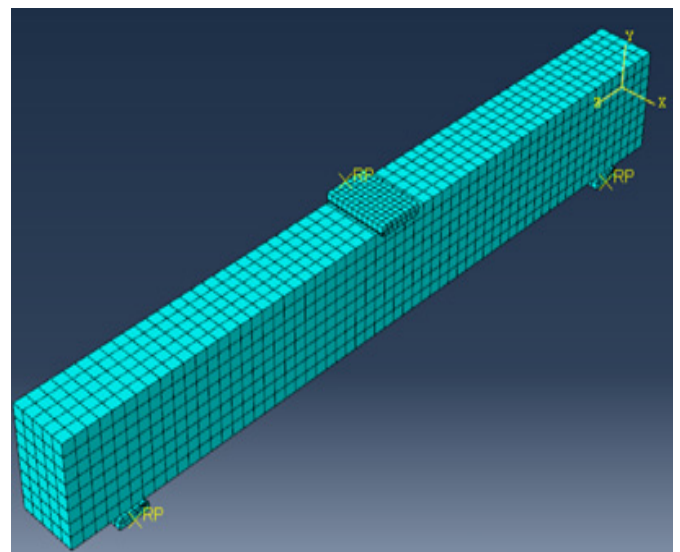
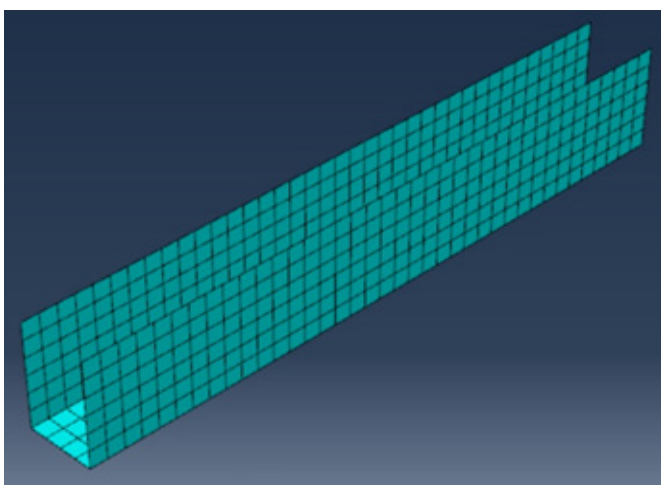
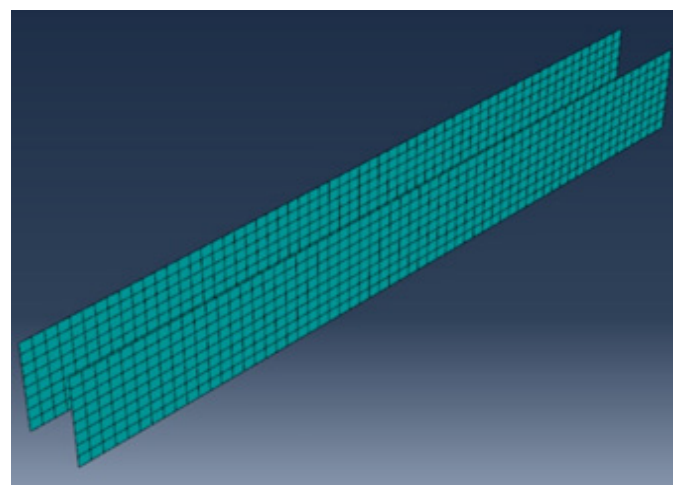


Figure 5: Meshed setup

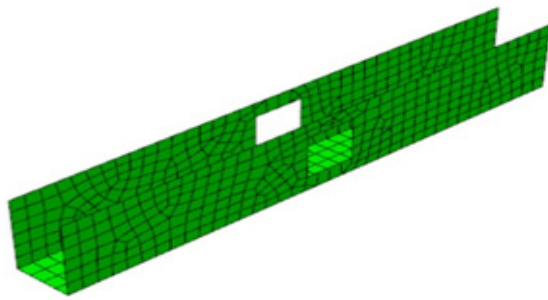


6-a: U shape wrapped CFRP

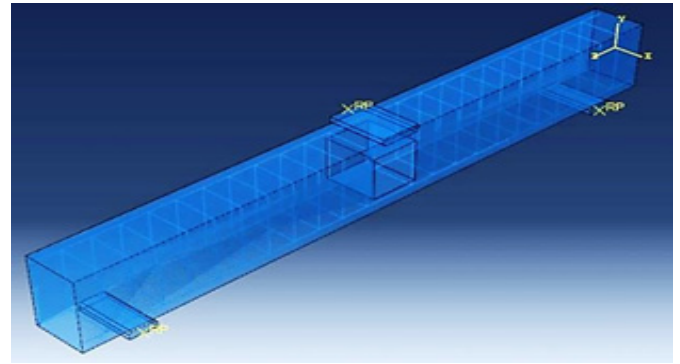


6-b: CFRP laminated 2- layers

Figure 6: Meshed CFRP laminates



7-a: mesh of CFRP laminates with opening



7-b: Design of CFRP laminates with opening

Figure 7: Design and mesh of CFRP laminates with opening

Design and mesh of CFRP laminates with opening shown in Fig.7. An increasing cyclic loading were applied on the beams with the specific time intervals until the failure of the beam. The main concrete part was considered as the important part for the failure. The loading curve is illustrated in Fig.8. Displacement for each cycle were chosen as 1.5 mm. Three rectangular web opening were used with different side sizes of 40%, 60%, and 75% of the depth in order to see the effect of web opening size on the flexural behavior of the beam for both cases of with and without CFRP. U shape wrapped CFRP were tie to the beam prior to simulation. The side sizes of the rectangular web openings were 12, 7.5, and 180 mm ,respectively. The boundary conditions were selected for both rigid bodies at sides of the beams as an ENCASTRE ($U_1=0, U_2=0, U_3=0, UR_1=0, UR_2=0, UR_3=0$) and friction were defined between the beam and rigid bodies in order to give the ability of moving in 2 directions to the beam on the supports. Loading were applied using

a displacement control loading via rigid body at the top of the beam and unload to the initial point and repeating this process.

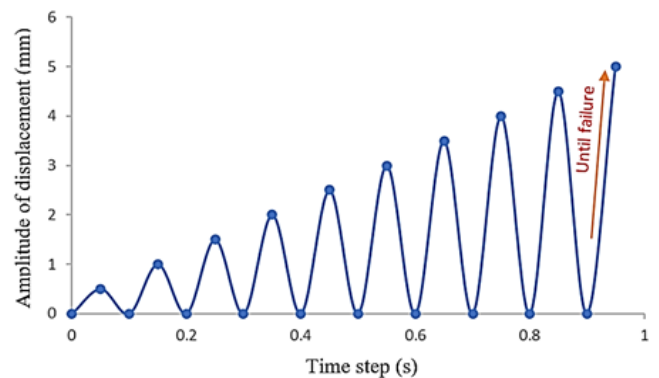


Figure 8: Amplitude of cyclic loading in different time steps of simulation

Table 4: Name and abbreviation of all conditions of the study

No.	Model Name	Abbreviation
1	RC Beam	RCB
2	RC Beam with web opening 40%	RCB-W40
3	RC Beam with web opening 60%	RCB-W60
4	RC Beam with web opening 75%	RCB-W75
5	RC Beam with 2-layer CFRP	RCB-CFRP-2L
6	RC Beam with 2-layer CFRP with web opening 40%	RCB-CFRP-2L-W40
7	RC Beam with 2-layer CFRP with web opening 60%	RCB-CFRP-2L-W60
8	RC Beam with 2-layer CFRP with web opening 75%	RCB-CFRP-2L-W75
9	RC Beam with U shape CFRP wrapped	RCB-CFRP-U
10	RC Beam with U shape CFRP wrapped with web opening 40%	RCB-CFRP-U-W40
11	RC Beam with U shape CFRP wrapped with web opening 60%	RCB-CFRP-U-W60
12	RC Beam with U shape CFRP wrapped with web opening 75%	RCB-CFRP-U-W75

RESULTS AND DISCUSSION

Fig. 9 demonstrates the effect of adding web opening on the flexural behavior of the RC beams with respect to the number of cyclic loading. It can be observed that with increasing the size of the web opening from 40% of the depth of the beam to 75%, the maximum von mises stress of the beam has reached to the maximum tensile strength of the beam at lower number of the cycles. Furthermore, stress concentration on the corner of the web opening may significantly decrease the strength of the beam. Fig.10. shows the start of the yielding on the concrete beam and increasing the number of the yielded elements throughout that in further cycles with increasing the displacement amplitude. The results of the simulation of the beam were in a good agreement with the literature in case of start of the yielding form the bottom part of the beams and propagating through the sample. Then with increasing the stress level at further cycles the top parts of the beam was also yield from the compressive stress

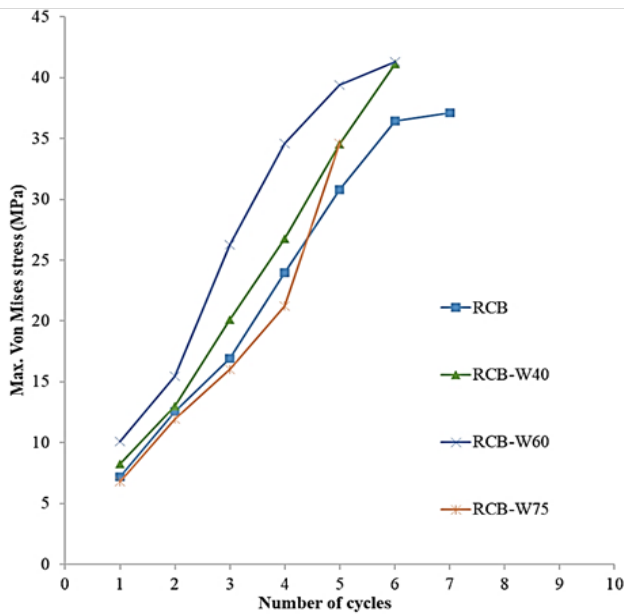


Figure 9: Maximum Von Mises stress of the RC beams with and without web opening at different cycles

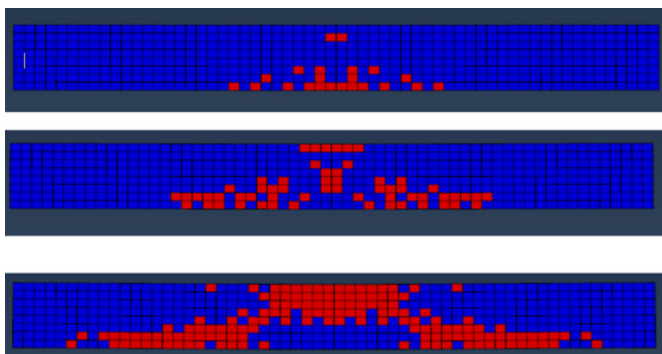


Figure 10: Yielding criteria stages on the RCB during the cyclic loading

The maximum von Mises stress distribution on the reinforced concrete beam after the fifth cycle was shown in Fig.11. It can be seen that the von Mises stress value has reached to about 40 MPa at the top center of the beam where the displacement has been applied via rigid body. The equivalent plastic strain on the concrete beam can be seen in Fig.12. In the figure it can be observed that the maximum PEEQ is at the compressive zone at the top of the beam and also at the bottom of the beam where the beam is under the tensile stress. With applying the displacement from the rigid bodies to the beam the compressive stress generates above the neutral line of the beam then the maximum plastic strain occurs on the zones that displacement directly applied.

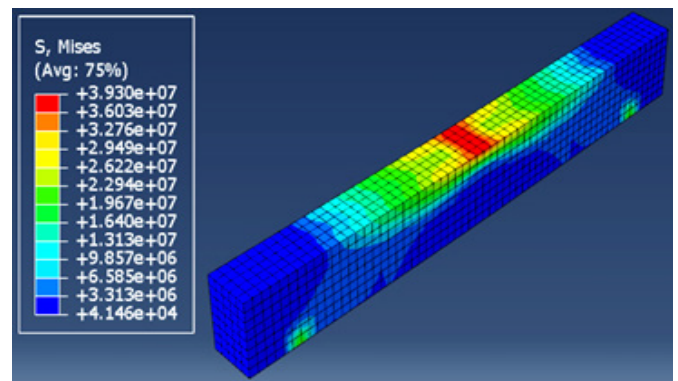


Figure 11: The maximum von Mises stress distribution on the reinforced concrete beam after the fifth cycle

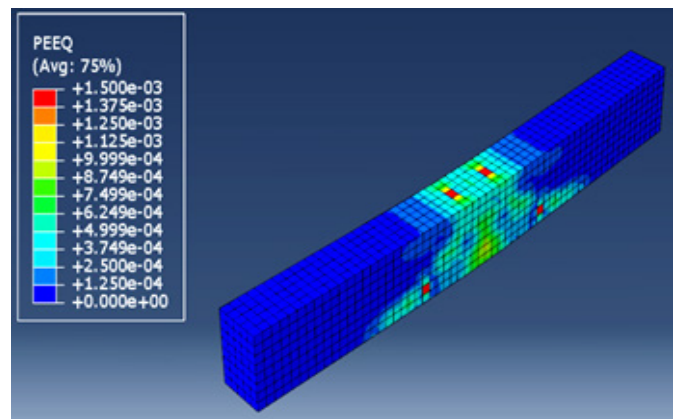


Figure 12: The equivalent plastic strain distribution on the reinforced concrete beam after the fifth cycle

Also, the von Mises stress distribution on the steel bars and stirrups is demonstrated in Fig. 13. As shown in Fig. 13, the most critical zone on the embedded region was the bottom bars where the maximum stress was 393.2 MPa and that was higher than the yield strength of the steel used in this model.

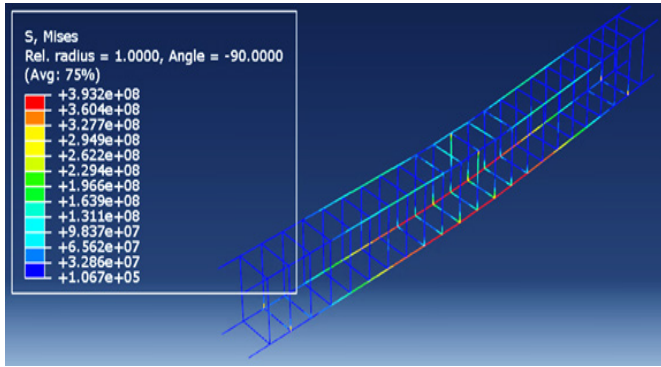


Figure 13: The maximum von Mises stress distribution on the reinforced concrete beam

With the addition of web opening on the stress distribution on the beam also has been observed for the case with CFRP. With the addition of web opening with different ratios of 40%, 60%, and 75%, it can be observed that the level of maximum von Mises stress after each cycle of loading was enhanced due to the stress concentration on the corners of the rectangular web openings and top of the opening. Fig. 14 and Fig.15 shows the maximum von Mises stress distribution on the RCB-W40, and RCB-W60 after the sixth cycle respectively.

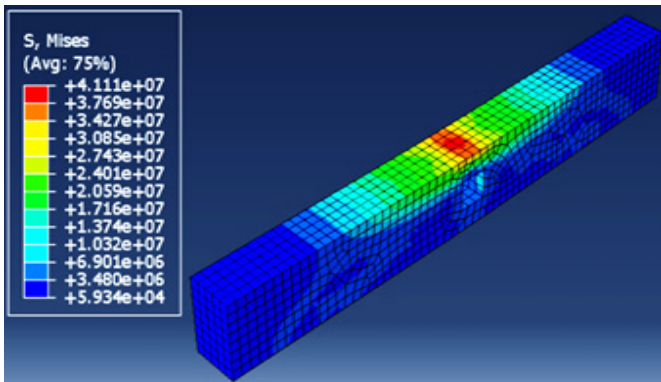


Figure 14: The maximum von Mises stress distribution on the RCB-W40 after the sixth cycle

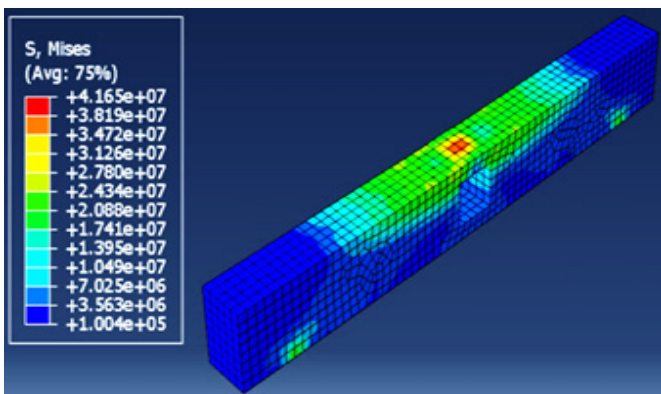


Figure 15: The maximum von Mises stress distribution on the RCB-W60 after the sixth cycle

Regarding the results of the Fig. 9, it can be observed that the level of maximum von Mises stress for RCB-W75 is lower than the others approximately at all the cycles. But this is related to the localization of deformation in this case and this case cannot be applicable for the beams. Fig. 16 and Fig. 17 show the results of equivalent plastic strain and deformation at the 4th cycle for RCB-W75, respectively. Fig. 18, 19 and 20 shows the Yielding criteria on the RCB-W40, RCB-W60 and RCB-W75 respectively and it can be seen that with increasing the size of the web openings the yielding zone is concentrated around the web opening at the center of the beam.

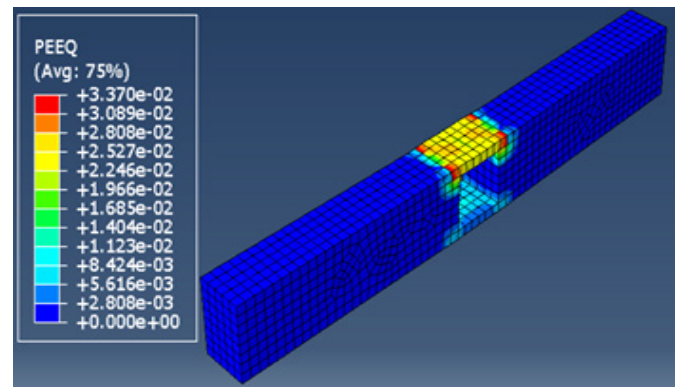


Figure 16: The equivalent plastic strain distribution on the RCB-W75 after the fourth cycle

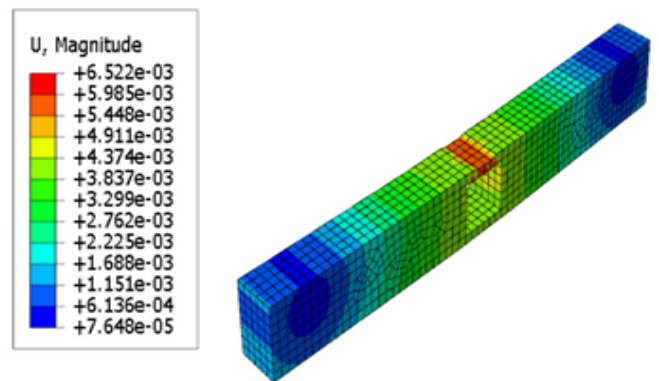


Figure 17: Localization of deformation on the top of the web opening part and failure of the RCB-W75 sample

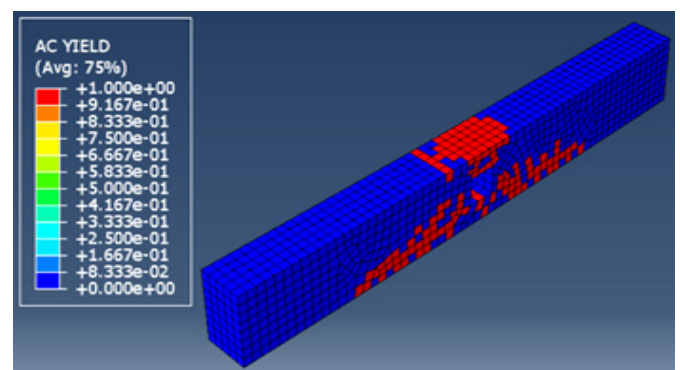


Figure 18: Yielding criteria on the RCB-W40

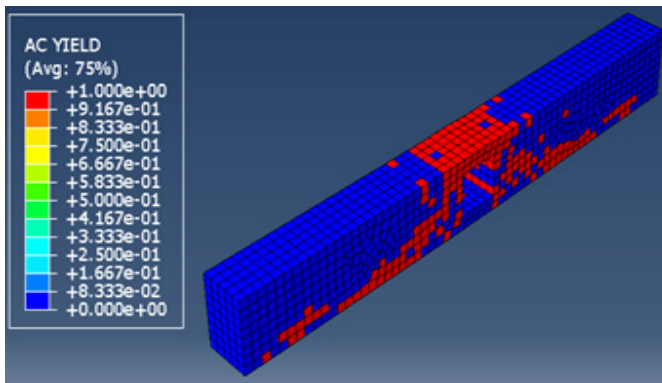


Figure 19: Yielding criteria on the RCB-W60

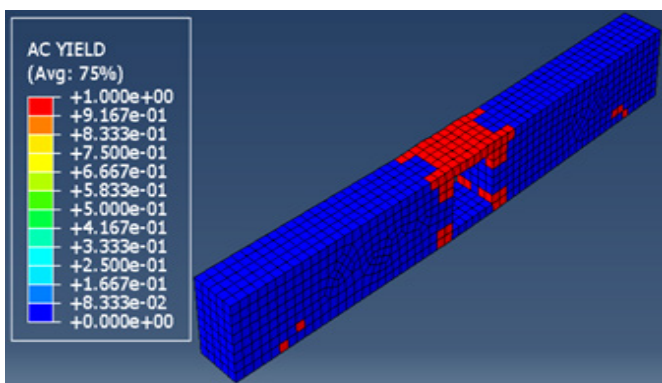


Figure 20: Yielding criteria on the RCB-W75

Reinforced with 2 layers of CFRP laminates at both side of the beam

The results of the flexural loading simulation of the beam reinforced by CFRP laminates at both sides is demonstrated in Fig. 21. With comparing the results of the simulation with 2 Layers of CFRP and without CFRP, it can be observed that for all the cases attachment of the CFRP has decreased the von Mises stress levels of each cycle. Also, considering the web openings with different sizes, it was asserted that the web opening caused to the failure faster than that of the case without the opening. Moreover, the yielding criteria for the beams with different web opening sizes has been demonstrated in Fig. 22-24. With comparing the results of the simulation for the RCB without the CFRP laminates and with CFRP laminates, it can be understood that the attachment of the CFRP layers has prevented the propagation of yielding to the most parts of the beam and in the beams with web openings it is mostly concentrated around the rectangular web opening sides, top, and corners. Furthermore, with increasing the size of the openings, this yielding becomes more concentrated on the center of the beam (see Fig. 24). Also, the maximum von Mises stress distribution on the CFRP laminates is depicted in Fig.25. It can be observed that the max von Mises level of 113 MPa was carried out by the CFRP layers to support the concrete beam under flexural loading.

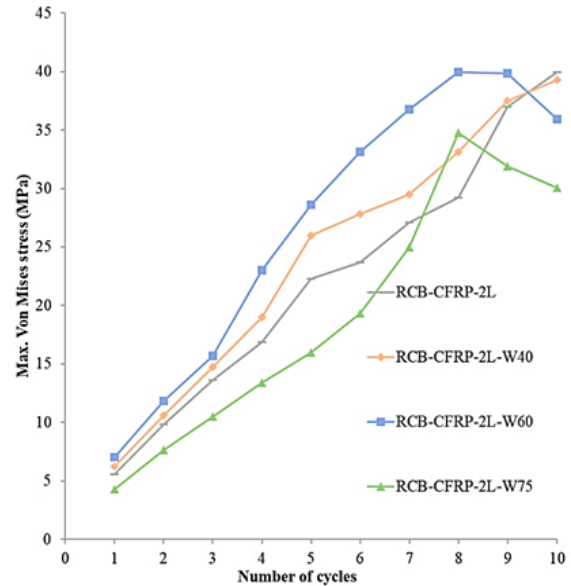


Figure 21: Maximum Von Mises stress of the RCB-CFRP-2L with and without web opening at different cycles

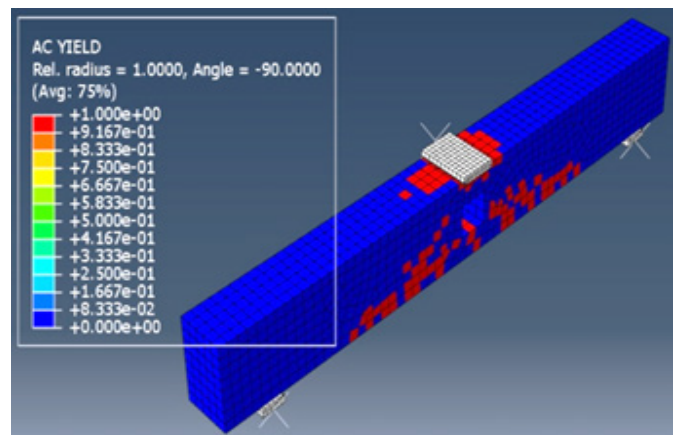


Figure 22: Yielding criteria on the RCB-CFRP-2L-W40

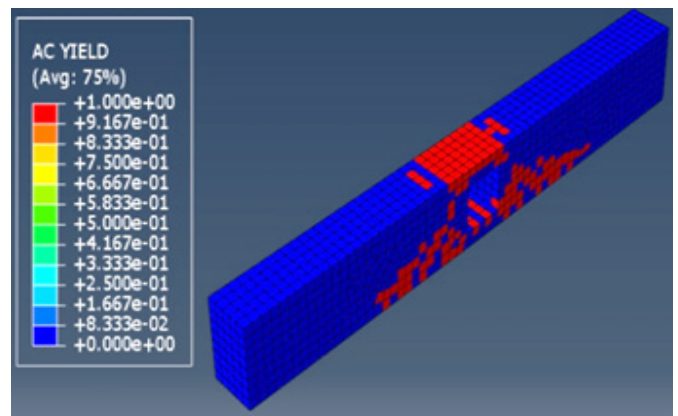


Figure 23: Yielding criteria on the RCB-CFRP-2L-W60

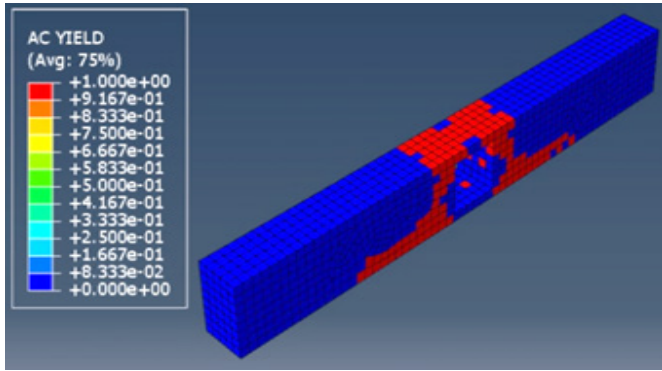


Figure 24: Yielding criteria on the RCB-CFRP-2L-W75

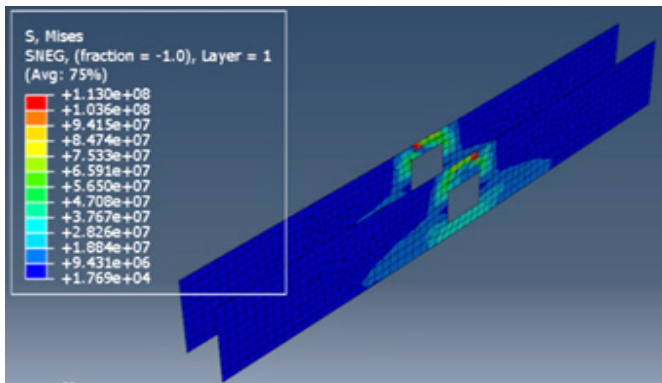


Figure 25: The maximum von Mises stress distribution on the CFRP laminates of RCB-CFRP-2L-W60

Reinforced with U shape CFRP around the beam

The results of the flexural loading simulation of the beam reinforced by U- shape CFRP is demonstrated in Fig. 26. Considering the results of the simulations shown in Fig. 21 and Fig. 26, it can be seen that the level of maximum Von Mises stress at each cycle for the U shape CFRP reinforced beams are lower than that of CFRP laminates reinforced beams. This is directly attributed to the significant effect of the bottom layer in U shape CFRP to prevent the initiation of the cracks on the bottom regions of the beam where the beam is under the tensile stress at these parts. Fig. 27 demonstrates the stress distribution of the RCB-CFRP-U beam without opening. Also, it can be seen in Fig. 27 that although, the maximum stress is at the top center of the beam, the load is more distributed to the other regions due to the attachment of the U shape CFRP to the RCB. After the 8th cycle, still the level of max von Mises stress is lower than 27 MPa after adding U shape CFRP to the beam. Also, yielding criteria of the RCB-CFRP-U is shown in Fig. 28. It can be observed that the beam started to fail from the bottom sides and top of the beam due to the tension loading and compressive loading, respectively. Fig. 29-31 demonstrates the start of the yielding on the beam at the center of the beam where the web opening with different sizes has been located. Also, it can be seen that with increasing the size of the web opening from 40% to 60% and

75%, the level of concentration on the top of the beam at the center has increased. This can be also related to the low strength of the concrete beam at the center due to the lack of stirrups at this zone where the load is just carried out by steel bars and concrete with the CFRP reinforcement.

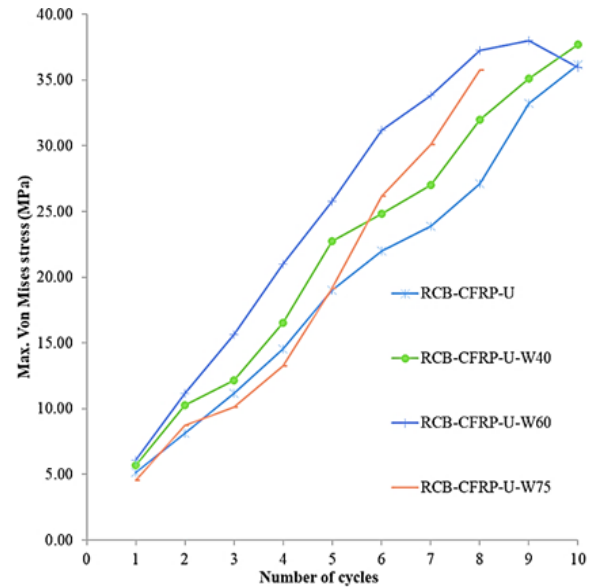


Figure 26: Maximum Von Mises stress of the RCB-CFRP-U with and without web opening at different cycles

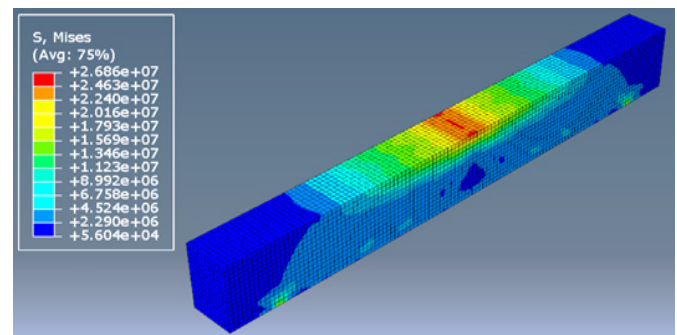


Figure 27: The maximum von Mises stress distribution on the RCB-CFRP-U after the 8th cycle

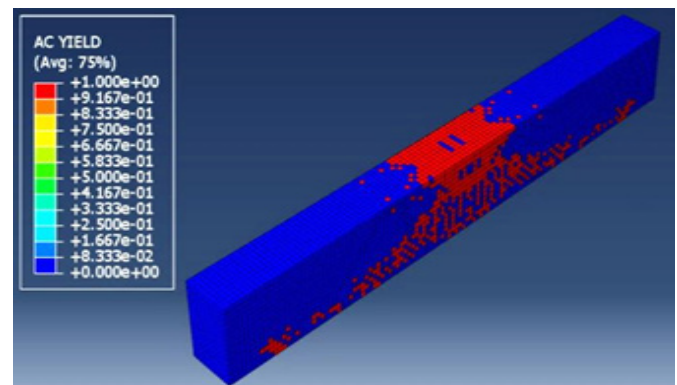


Figure 28: Yielding criteria of the RCB-CFRP-U under the flexural loading

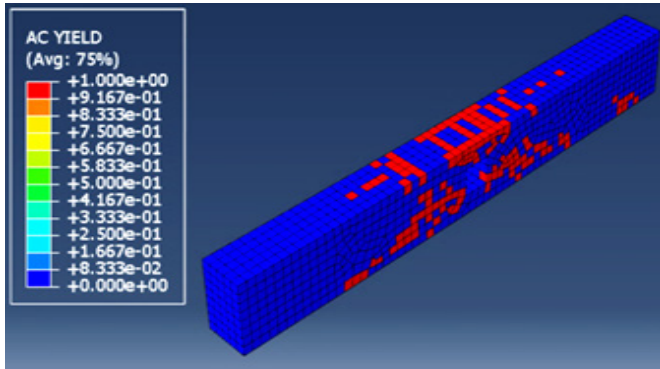


Figure 29: Yielding criteria of the RCB-CFRP-U-W40

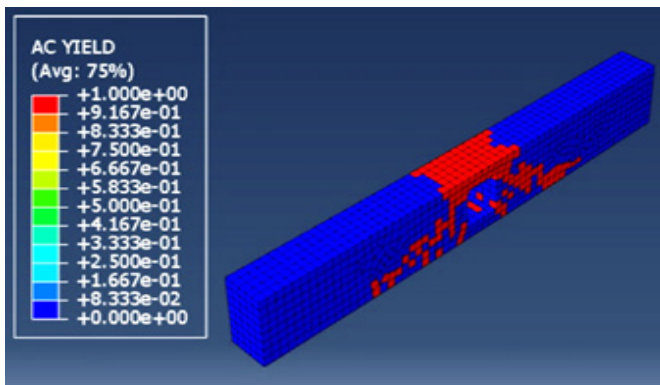


Figure 30: Yielding criteria on the RCB-CFRP-U-W60

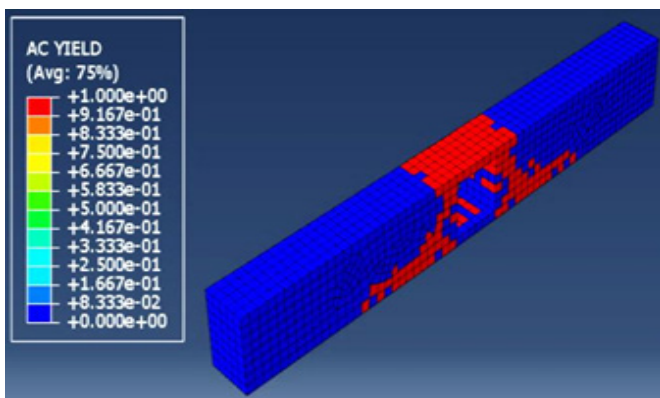


Figure 31: Yielding criteria on the RCB-CFRP-U-W75

CONCLUSIONS

In the current paper, the effect of CFRP on the flexural behavior of RC beams were investigated using ABAQUS software. Furthermore, the effect of web opening with different sizes were analyzed and the some of the results are as follow:

1. Two layers CFRP laminates increased the flexural strength of the RC beams under cyclic loading significantly.

2. With changing the shape of the CFRP laminates to a U shape CFRP layer, the number of cycles to failure were increased and von Mises stress level at each cycle were also decreased.
3. 3. With increasing the size of the web opening, the flexural strength of both RCB and RCB-CFRP was decreased gradually. Moreover, deformation localization was seen on the samples with 75% web opening size which caused to the failure of the beam at earlier cycles.
4. 4. it can be seen that the level of maximum Von Mises stress at each cycle for the U shape CFRP reinforced beams are lower than that of CFRP laminates reinforced beams.
5. 5. All beams yield from the bottom parts due to the lower strength of the concrete against the tension loading. However, with adding web openings to the beams, the stress concentration was occurred on the edges and top of the web opening.

ACKNOWLEDGEMENTS

"The authors would like to thank Mustansiriyah University (www.uomustansiriyah.edu.iq) Baghdad-Iraq for its support in the present work".

REFERENCES

1. Mansur, M. (2006). Design of reinforced concrete beams with web openings. Proceedings of the 6th Asia-Pacific structural engineering and construction conference (ASPEC 2006), Kuala Lumpur, Malaysia. 5–6 September 2006. P.104–120.
2. Mansur, M.A. (1998). Effect of openings on the behavior and strength of R/C beams in shear. Cement and Concrete Composites, Elsevier Science Ltd., Vol. 20, No.6, 477-486, Doi:10.1016/S0958-9465(98)00030-4
3. Mitali, R. P., and Gajjar, R. K. (2012). Shear Strengthening of RC Beams using CFRP. International Journal of Advanced Engineering Technology, Vol. 3, No. 1, PP. 338-342.
4. Abdulrahman MB, Al-Jaberi LA, Hasan SS. (2021). The Effect of Opening Size and Location on the Performance of Reinforced Concrete T-Beams under Pure Torque. Tikrit Journal of Engineering Sciences, 28 (1), 46- 53.
5. Ahmed, A., Fayyadh, M. M., Naganathan, S., & Nasharuddin, K. (2012). Reinforced concrete beams with web openings: A state of the art review. Materials & Design, 40, 90-102.
6. Aykac, B., Kalkan, I., Aykac, S., & Egriboz, Y. E. (2013). Flexural behavior of RC beams with regular square or circular web openings. Engineering Structures, 56, 2165-2174.

7. Yang, K. H., Eun, H. C., & Chung, H. S. (2006). The influence of web openings on the structural behavior of reinforced high-strength concrete deep beams. *Engineering Structures*, 28(13), 1825-1834.
8. Yoo, T. M. (2011). *Strength and behaviour of high strength concrete deep beam with web openings*. Nathan: Griffith University.
9. Chin, S. C., N. Shafiq and M. F. Nuruddin. (2015). FRP as strengthening material for Reinforced Concrete beams with openings: A review. *KSCE Journal of Civil Engineering* 19(1): 213-219.
10. Djeddi, F., Y. Ghernouti, Y. Abdelaziz and L. Alex. (2016). Strengthening in flexure-shear of RC beams with hybrid FRP systems: Experiments and numerical modeling. *Journal of Reinforced Plastics and Composites* 35(22): 1642-1660.
11. Osman, B. H., Wu, E., Ji, B., & Abdelgader, A. M. (2016). A state of the art review on reinforced concrete beams with openings retrofitted with FRP. *International Journal of Advanced Structural Engineering*, 8(3), 253-267.
12. Uji, K. (1992). Improving shear capacity of existing reinforced concrete members by applying carbon fiber sheets. *Transactions of the Japan Concrete Institute* 14.
13. Malek, A. M. (1998). Ultimate shear capacity of reinforced concrete beams strengthened with web-bonded fiber-reinforced plastic plates. *ACI Structural Journal* 95(4): 391-399.
14. Triantafillou, T. C. (1998). Shear strengthening of reinforced concrete beams using epoxy-bonded FRP composites. *ACI structural journal* 95: 107-115.
15. Bernaert, S. and C. P. Siess (1956). *Strength in Shear of Reinforced Concrete Beams under Uniform Load*, University of Illinois Engineering Experiment Station.
16. Elgabbas, F., Ahmed, E. A., & Benmokrane, B. (2017). Flexural behavior of concrete beams reinforced with ribbed basalt-FRP bars under static loads. *Journal of Composites for Construction*, 21(3), 04016098.
17. ACI 318-14. (2014). *Building Code Requirements for Structural Concrete (ACI 318-14)* American Concrete Institute; Farmington Hills, MI, USA: 2014. p. 524.
18. Rabinovitch, O. and Y. Frostig. (2003). Experiments and analytical comparison of RC beams strengthened with CFRP composites. *Composites part B: engineering* 34(8): 663-677.
19. Akbarzadeh, H. and A. Maghsoudi. (2010). Experimental and analytical investigation of reinforced high strength concrete continuous beams strengthened with fiber reinforced polymer. *Materials & Design* 31(3): 1130-1147.
20. Hawileh, R. A., T. A. El-Maaddawy and M. Z. Naser. (2012). Nonlinear finite element modeling of concrete deep beams with openings strengthened with externally-bonded composites. *Materials & Design* 42: 378-387.
21. Al-Tersawy, S. H. (2013). Effect of fiber parameters and concrete strength on shear behavior of strengthened RC beams. *Construction and Building Materials* 44: 15-24.
22. Sonnenschein, R., K. Gajdosova and I. Holly. (2016). FRP Composites and their Using in the Construction of Bridges. *Procedia Engineering* 161: 477-482.
23. De Lorenzis, L. and A. Nanni (2001). "Shear Strengthening of Reinforced Concrete Beams with Near-Surface Mounted Fibre Reinforced Polymer." *ACI Structural Journal* 98.
24. ABAQUS, U. s. M. and C. U. s. Manual. (2012). *Dasault Systemes Simulia Corp. Providence, RI, USA* 6(1). A.S.U.s.
25. 25. Manual, Abaqus 6.11, [http://130.149.89\(2080\)\(2012\)v6](http://130.149.89(2080)(2012)v6).
26. Lee, J., & Fenves, G. L. (1998). Plastic-damage model for cyclic loading of concrete structures. *Journal of engineering mechanics*, 124(8), 892-900.
27. S. Bahij, S.K. Adekunle, M. Al-Osta, S. Ahmad, S.U. Al-Dulaijan, M.K. Rahman. (2018). Numerical investigation of the shear behavior of reinforced ultra-high-performance concrete beams. *Structural Concrete* 19(1), 305-317.
28. Saqan, E. I., H. A. Rash-eed and R. A. Hawileh. (2013). An efficient design procedure for flexural strengthening of RC beams based on ACI 440.2R-08. *Composites Part B: Engineering* 49: 71-79.
29. ACI Committee 440.1R. (2006). *Guide for the Design and Construction of Structural Concrete Reinforced with FRP Bars*, ACI Manual of Concrete Practice, American Concrete Institute, Farming Hills, USA.
30. ACI Committee 440.2R. (2008). *Guide for the Design and Construction of Externally Bonded FRP Systems for Strengthening Concrete Structures*, American Concrete Institute, Detroit, USA.
31. M. Barbato. (2009). Efficient finite element modelling of reinforced concrete beams retrofitted with fibre reinforced polymers. *Computers & Structures* 87(3-4), 167-176.

Paper submitted: 10.07.2021.

Paper accepted: 18.08.2021.

*This is an open access article distributed under the
CC BY 4.0 terms and conditions.*